J. KSIAM Vol.20, No.2, 137–150, 2016 http://dx.doi.org/10.12941/jksiam.2016.20.137

ROBUST A POSTERIORI ERROR ESTIMATOR FOR LOWEST-ORDER FINITE ELEMENT METHODS OF INTERFACE PROBLEMS

KWANG-YEON KIM

DEPARTMENT OF MATHEMATICS, KANGWON NATIONAL UNIVERSITY, CHUNCHEON, SOUTH KOREA
E-mail address: eulerkim@kangwon.ac.kr

ABSTRACT. In this paper we analyze an a posteriori error estimator based on flux recovery for lowest-order finite element discretizations of elliptic interface problems. The flux recovery considered here is based on averaging the discrete normal fluxes and/or tangential derivatives at midpoints of edges with weight factors adapted to discontinuous coefficients. It is shown that the error estimator based on this flux recovery is equivalent to the error estimator of Bernardi and Verfürth based on the standard edge residuals uniformly with respect to jumps of the coefficient between subdomains. Moreover, as a byproduct, we obtain slightly modified weight factors in the edge residual estimator which are expected to produce more accurate results.

1. INTRODUCTION

Let $\Omega \subset \mathbb{R}^2$ be an open bounded polygonal domain with the boundary $\partial\Omega = \overline{\Gamma_D \cup \Gamma_N}$, $\Gamma_D \cap \Gamma_N = \emptyset$. We consider the second-order elliptic equation

$$-\nabla \cdot (\alpha \nabla u) = f \quad \text{in } \Omega \tag{1.1}$$

subject to the boundary conditions

$$u = u_D \quad \text{on } \Gamma_D, \qquad (\alpha \nabla u) \cdot \boldsymbol{n} = g_N \quad \text{on } \Gamma_N, \tag{1.2}$$

where the diffusion coefficient α is a positive scalar-valued function and $\boldsymbol{n}$ denotes the outward unit normal vector on $\partial\Omega$.

The variational formulation of the problem (1.1)–(1.2) is to find $u \in H^1(\Omega)$ such that $u = u_D$ on Γ_D and

$$\int_\Omega \alpha \nabla u \cdot \nabla v \, d\boldsymbol{x} = \int_\Omega f v \, d\boldsymbol{x} + \int_{\Gamma_N} g_N v \, ds \qquad \forall v \in H^1_D(\Omega), \tag{1.3}$$

where

$$H^1_D(\Omega) = \{v \in H^1(\Omega) : v = 0 \text{ on } \Gamma_D\}.$$

We assume that the coefficient α is piecewise constant with respect to a partition of the domain Ω into disjoint polygonal subdomains $\{\Omega_i\}_{i=1}^n$ and may have large jumps between

Received by the editors March 24 2016; Revised June 15 2016; Accepted in revised form June 15 2016; Published online June 20 2016.

2000 *Mathematics Subject Classification.* 65N15, 65N30.

Key words and phrases. a posteriori error estimator, finite element method, interface problem, flux recovery.

subdomains. In this case the problem (1.1)–(1.2) is often referred to as an *interface problem*, and it is important to observe that the following continuity conditions hold across the edges of the triangulation:

(NC) The normal flux $\alpha\nabla u \cdot \boldsymbol{n}$ is continuous across the edges, i.e.,

$$\alpha\nabla u \in H(\mathrm{div};\Omega) = \{\boldsymbol{\tau} \in (L^2(\Omega))^2 : \nabla\cdot\boldsymbol{\tau} \in L^2(\Omega)\}.$$

(TC) The tangential derivative $\nabla u \cdot \boldsymbol{t}$ is continuous across the edges, i.e.,

$$\nabla u \in H(\mathrm{curl};\Omega) = \{\boldsymbol{\tau} \in (L^2(\Omega))^2 : \mathrm{curl}\,\boldsymbol{\tau} \in L^2(\Omega)\}.$$

Notice also that neither $\nabla u \cdot \boldsymbol{n}$ nor $\alpha\nabla u \cdot \boldsymbol{t}$ is continuous across the edges where α has a jump. This implies that the global regularity of the solution u is at best $H^{\frac{3}{2}-\epsilon}(\Omega)$ for any $\epsilon > 0$.

In this paper we deal with three lowest-order finite element methods, namely, the $P1$ conforming/nonconforming FEMs and the lowest-order Raviart–Thomas (RT_0) mixed FEM over triangular meshes. One popular tool for efficient implementation of finite element methods is adaptive mesh refinement guided by an a posterior error estimator which can provide quantitative and/or qualitative information on the numerical error. An error estimator for the interface problem (1.1)–(1.2) consisting of standard element and edge residuals was first proposed by Bernardi and Verfürth [1] for the $P1$ conforming FEM; see also [2]. The key result is that appropriate weight factors depending on α should be incorporated into the residuals in order for the error estimator to be robust with respect to the jumps of α between subdomains. Moreover, following the technique of [3] for the Poisson equation, Cai and Zhang [4, 5] showed that element residuals are redundant, i.e., edge residuals dominate even for the interface problem (1.1)–(1.2).

Since the pioneering work of Zienkiewicz and Zhu [6], the error estimator based on gradient (∇u) or flux ($\alpha\nabla u$) recovery has been widely used and well investigated. The most popular recovery procedure in the lowest-order FEMs is based on averaging either the flux or gradient at *vertices* of the triangulation (cf. [6, 7]). Gradient recovery by averaging at *midpoints of edges* was discussed in [8, 9] for the $P1$ conforming FEM, in Brandts [10] for the RT_0 mixed FEM and then in [11] for the $P1$ nonconforming FEM. In either way the recovered flux or gradient is a piecewise linear polynomial and is superconvergent under favorable conditions (such as uniform triangulations and smooth solutions), in which case we get the asymptotically exact error estimator. But the error estimator is not well-suited for the interface problem, as illustrated by the numerical results of [4, 5]. On the other hand, in consideration of the two continuity conditions (NC) and (TC) stated above, Cai and Zhang [4, 5] recently proposed an error estimator using flux recovery in $H(\mathrm{div};\Omega)$ and/or gradient recovery in $H(\mathrm{curl};\Omega)$ which is achieved either globally (and implicitly) by the L^2 projection or locally (and explicitly) by averaging on edges with weight factors depending on the coefficient α. Numerical results in [4, 5] show that the error estimator using the explicit recovery is fairly accurate but not asymptotically exact even under the most favorable conditions.

In this paper we adapt the recovery procedure based on averaging at midpoints of edges to the interface problem (1.1)–(1.2), inspired by the works of Cai and Zhang [4, 5]. The adapted

procedure recovers the flux variable, but it also involves gradient recovery to reflect the continuity of the tangential derivative. More specifically, we combine flux averaging in the normal direction and gradient averaging in the tangential direction at the midpoint of each edge to construct a piecewise linear flux approximation (but not in $H(\mathrm{div};\Omega)$). This flux recovery is applicable to the $P1$ conforming/nonconforming FEMs and the RT_0 mixed FEM in a unified way, and we show that the error estimator based on the recovered flux is equivalent to the edge residual error estimator of Bernardi and Verfürth uniformly with respect to the jumps of the coefficient α between subdomains. In fact, it turns out that our recovery-based error estimator is nothing but the edge residual error estimator with slightly modified weight factors. Thus this error estimator is not only robust with respect to the jumps of α between subdomains (under the monotonicity condition of Bernardi and Verfürth), but also expected to be as inexpensive as and more accurate than the edge residual error estimator.

The remainder of the paper is organized as follows. In Section 2 we introduce some notation to be used throughout the paper and define the three lowest-order FEMs. In Section 3 we review the edge residual error estimators for the interface problem. In Section 4 we present the flux recovery based on averaging at midpoints of edges and the corresponding error estimator which is shown to be uniformly equivalent to the edge residual error estimator. Finally, in Section 5, some numerical results are provided to illustrate the performance of our error estimator.

2. Notation and Finite Element Methods

Let $\mathcal{T}_h = \{T\}$ be a shape-regular triangulation of Ω into triangular elements such that $\overline{\Omega} = \bigcup_{T\in\mathcal{T}_h} T$, where $h_T = \mathrm{diam}(T)$ and $h = \max_{T\in\mathcal{T}_h} h_T$. It is assumed that the subdomain interface $\Gamma_s := \left(\bigcup_{i=1}^n \partial\Omega_i\right) \setminus \partial\Omega$ is aligned with the triangulation $\mathcal{T}_h$, i.e., Γ_s does not pass through the interior of any element $T \in \mathcal{T}_h$.

We denote the collection of all vertices of $\mathcal{T}_h$ by $\mathcal{N}_h = \{\boldsymbol{z}\}$ and the collection of all edges of $\mathcal{T}_h$ by $\mathcal{E}_h = \{e\}$, where $h_e = \mathrm{diam}(e)$. For a vertex $\boldsymbol{z} \in \mathcal{N}_h$, let $\omega_{\boldsymbol{z}}$ be the union of all elements of $\mathcal{T}_h$ sharing $\boldsymbol{z}$. For an edge $e \in \mathcal{E}_h$, let ω_e be the union of at most two elements of $\mathcal{T}_h$ sharing e. We set $\omega_e = T_e^+ \cup T_e^-$ for an interior edge e and $\omega_e = T_e$ for a boundary edge e.

With each edge $e \in \mathcal{E}_h$, we associate a fixed unit normal vector $\boldsymbol{n}_e = (n_1, n_2)$ and a unit tangent vector $\boldsymbol{t}_e = (-n_2, n_1)$ such that $\boldsymbol{n}_e$ is oriented from T_e^+ to T_e^- for an interior edge e and is outward to T_e for a boundary edge e. For a piecewise smooth function v, we define the jump of v across an interior edge e as

$$[\![v]\!]_e = v|_{T_e^+} - v|_{T_e^-},$$

where the index e is suppressed whenever there is no confusion.

The restriction of α to an element $T \in \mathcal{T}_h$ is denoted by $\alpha_T \equiv \alpha|_T$. Let $\bar{f}_S := \frac{1}{|S|}\int_S f\,d\boldsymbol{x}$, where $|S|$ is the area of a domain $S \subset \mathbb{R}^2$, and let $\bar{f}_h$ be the piecewise constant function such that $\bar{f}_h|_T \equiv \bar{f}_T$ for all $T \in \mathcal{T}_h$. The notation ∇_h represents the gradient operator taken piecewise over the triangulation $\mathcal{T}_h$.

Now we define the lowest-order FEMs for the problem (1.1)–(1.2). Let $\mathbb{P}_k(T)$ be the space of all polynomials of degree at most k on an element T. Based on the variational formulation

(1.3), the $P1$ conforming FEM is to find $u_h^c \in S_h^c$ such that $u_h^c(\boldsymbol{z}) = u_D(\boldsymbol{z})$ at each vertex $\boldsymbol{z} \in \mathcal{N}_h \cap \Gamma_D$ and

$$\int_\Omega \alpha \nabla u_h^c \cdot \nabla v_h \, d\boldsymbol{x} = \int_\Omega f v_h \, d\boldsymbol{x} + \int_{\Gamma_N} g_N v_h \, ds \qquad \forall v_h \in S_{h,D}^c, \tag{2.1}$$

where

$$\begin{aligned} S_h^c &= \{v_h \in H^1(\Omega) : v_h|_T \in \mathbb{P}_1(T) \ \ \forall T \in \mathcal{T}_h\}, \\ S_{h,D}^c &= \{v_h \in S_h^c : v_h|_{\Gamma_D} = 0\}. \end{aligned}$$

Similarly, the $P1$ nonconforming FEM is to find $u_h^{nc} \in S_h^{nc}$ such that $\int_e u_h^{nc} \, ds = \int_e u_D \, ds$ for each edge $e \subset \Gamma_D$ and

$$\int_\Omega \alpha \nabla_h u_h^{nc} \cdot \nabla_h v_h \, d\boldsymbol{x} = \int_\Omega f v_h \, d\boldsymbol{x} + \int_{\Gamma_N} g_N v_h \, ds \qquad \forall v_h \in S_{h,D}^{nc}, \tag{2.2}$$

where

$$\begin{aligned} S_h^{nc} &= \left\{ v_h \in L^2(\Omega) : v_h|_T \in \mathbb{P}_1(T) \ \ \forall T \in \mathcal{T}_h \text{ and } \int_e [\![v_h]\!] \, ds = 0 \text{ for each edge } e \subset \Omega \right\}, \\ S_{h,D}^{nc} &= \left\{ v_h \in S_h^{nc} : \int_e v_h \, ds = 0 \text{ for each edge } e \subset \Gamma_D \right\}. \end{aligned}$$

On the other hand, the RT_0 mixed FEM is based on the first-order mixed system of the problem (1.1)–(1.2) having the form

$$\boldsymbol{\sigma} = \alpha \nabla u, \quad \nabla \cdot \boldsymbol{\sigma} = -f \quad \text{in } \Omega, \qquad u|_{\Gamma_D} = u_D, \quad \boldsymbol{\sigma} \cdot \boldsymbol{n}|_{\Gamma_N} = g_N,$$

and is given as follows: find $(\boldsymbol{\sigma}_h^m, u_h^m) \in RT_h \times W_h$ such that $\int_e \boldsymbol{\sigma}_h^m \cdot \boldsymbol{n}_e \, ds = \int_e g_N \, ds$ for each edge $e \subset \Gamma_N$ and

$$\begin{cases} \displaystyle\int_\Omega \alpha^{-1} \boldsymbol{\sigma}_h^m \cdot \boldsymbol{\tau}_h \, d\boldsymbol{x} + \int_\Omega \nabla \cdot \boldsymbol{\tau}_h \, u_h^m \, d\boldsymbol{x} = \int_{\Gamma_D} u_D \, \boldsymbol{\tau}_h \cdot \boldsymbol{n} \, ds \qquad \forall \boldsymbol{\tau}_h \in RT_{h,N}, \\ \displaystyle\int_\Omega \nabla \cdot \boldsymbol{\sigma}_h^m \, w_h \, d\boldsymbol{x} = -\int_\Omega f w_h \qquad \forall w_h \in W_h, \end{cases} \tag{2.3}$$

where

$$\begin{aligned} RT_h &= \{\boldsymbol{\tau}_h \in H(\mathrm{div}; \Omega) : \boldsymbol{\tau}_h|_T \in (\mathbb{P}_0(T))^2 + \boldsymbol{x}\mathbb{P}_0(T) \ \ \forall T \in \mathcal{T}_h\}, \\ RT_{h,N} &= \{\boldsymbol{\tau}_h \in RT_h : \boldsymbol{\tau}_h \cdot \boldsymbol{n}|_{\Gamma_N} = 0\}, \\ W_h &= \{w_h \in L^2(\Omega) : w_h|_T \in \mathbb{P}_0(T) \ \ \forall T \in \mathcal{T}_h\}. \end{aligned}$$

Finally, C will stand for a positive generic constant which is independent of the jumps of α between subdomains as well as the mesh size h.

3. EDGE RESIDUAL ERROR ESTIMATORS

From now on we assume for simplicity that u_D is continuous and piecewise linear over Γ_D and g_N is piecewise constant over Γ_N.

Suppose that the flux approximation $\boldsymbol{\sigma}_h \approx \boldsymbol{\sigma} = \alpha\nabla u$ has been obtained from one of the lowest-order FEMs as follows:

(a) $\boldsymbol{\sigma}_h = \alpha\nabla u_h^c$, where u_h^c is the solution of the $P1$ conforming FEM (2.1) such that $u_h^c|_{\Gamma_D} = u_D$. Note that the discrete tangential derivative $\alpha^{-1}\boldsymbol{\sigma}_h \cdot \boldsymbol{t}_e$ is continuous across interior edges of $\mathcal{T}_h$, but the discrete normal flux $\boldsymbol{\sigma}_h \cdot \boldsymbol{n}_e$ is not.

(b) $\boldsymbol{\sigma}_h = \alpha\nabla_h u_h^{nc}$, where u_h^{nc} is the solution of the $P1$ nonconforming FEM (2.2). Note that neither the discrete tangential derivative $\alpha^{-1}\boldsymbol{\sigma}_h \cdot \boldsymbol{t}_e$ nor the discrete normal flux $\boldsymbol{\sigma}_h \cdot \boldsymbol{n}_e$ is continuous across interior edges of $\mathcal{T}_h$.

(c) $\boldsymbol{\sigma}_h = \boldsymbol{\sigma}_h^m$, where $\boldsymbol{\sigma}_h^m$ is the vector solution of the RT_0 mixed FEM (2.3) such that $\boldsymbol{\sigma}_h^m \cdot \boldsymbol{n}|_{\Gamma_N} = g_N$. Note that the discrete normal flux $\boldsymbol{\sigma}_h \cdot \boldsymbol{n}_e$ is continuous across interior edges of $\mathcal{T}_h$, but the discrete tangential derivative $\alpha^{-1}\boldsymbol{\sigma}_h \cdot \boldsymbol{t}_e$ is not.

Using the flux approximation $\boldsymbol{\sigma}_h$ obtained as above, we define the following error estimator based on edge residuals (cf. [1, 2, 3, 4, 5])

$$\eta_E = \left(\sum_{e \in \mathcal{E}_h} \eta_e^2 \right)^{1/2}$$

with

$$\eta_e^2 = \begin{cases} \dfrac{2}{\alpha_{T_e^+} + \alpha_{T_e^-}} h_e \|[\![\boldsymbol{\sigma}_h \cdot \boldsymbol{n}_e]\!]\|_{0,e}^2 + \dfrac{2\alpha_{T_e^+}\alpha_{T_e^-}}{\alpha_{T_e^+} + \alpha_{T_e^-}} h_e \|[\![\alpha^{-1}\boldsymbol{\sigma}_h \cdot \boldsymbol{t}_e]\!]\|_{0,e}^2 & \text{for } e \subset \Omega, \\ \alpha_{T_e} h_e \|(\alpha^{-1}\boldsymbol{\sigma}_h)|_{T_e} \cdot \boldsymbol{t}_e - \frac{du_D}{ds}\|_{0,e}^2 & \text{for } e \subset \Gamma_D, \\ \alpha_{T_e}^{-1} h_e \|\boldsymbol{\sigma}_h|_{T_e} \cdot \boldsymbol{n}_e - g_N\|_{0,e}^2 & \text{for } e \subset \Gamma_N, \end{cases}$$

where $\frac{dw}{ds}\big|_e$ denotes the directional derivative of $w|_e$ in the direction of $\boldsymbol{t}_e$. We remark that the local contribution η_e vanishes for all $e \subset \Gamma_D$ when $\boldsymbol{\sigma}_h$ is computed from the $P1$ conforming FEM and vanishes for all $e \subset \Gamma_N$ when $\boldsymbol{\sigma}_h$ is computed from the RT_0 mixed FEM. (It does not vanish but becomes a higher-order term if u_D is not piecewise linear and/or g_N is not piecewise constant.)

The weight factor $\frac{2}{\alpha_{T_e^+}+\alpha_{T_e^-}}$ (which is equivalent to $\frac{1}{\max\{\alpha_{T_e^+},\alpha_{T_e^-}\}}$) for the normal jump $h_e\|[\![\boldsymbol{\sigma}_h \cdot \boldsymbol{n}_e]\!]\|_{0,e}^2$ was first presented in [1] for the $P1$ conforming FEM and the weight factor $\frac{2\alpha_{T_e^+}\alpha_{T_e^-}}{\alpha_{T_e^+}+\alpha_{T_e^-}}$ (which is equivalent to $\min\{\alpha_{T_e^+}, \alpha_{T_e^-}\}$) for the tangential jump $h_e\|[\![\alpha^{-1}\boldsymbol{\sigma}_h \cdot \boldsymbol{t}_e]\!]\|_{0,e}^2$ was adopted in [12] to control the jump $h_e^{-1}\|[\![u_h^{nc}]\!]\|_{0,e}^2$ for the $P1$ nonconforming FEM. With these weight factors, the error estimator η_E is reliable and efficient independently of the jumps of the coefficient α between subdomains under the following condition stated in [1].

Monotonicity Condition: For any two different subdomains Ω_i and Ω_j, which share at least one point, there is a connected path from Ω_i to Ω_j through adjacent subdomains such that the coefficient α is monotone along this path.

When this condition is satisfied, we can obtain the robust global upper bound (extending the result of [4, 5] to the nonhomogeneous case $u_D \neq 0$, $g_N \neq 0$)

$$\|\alpha^{-1/2}(\boldsymbol{\sigma} - \boldsymbol{\sigma}_h)\|_{0,\Omega} \leq C(\eta_E + H_f) \tag{3.1}$$

with the extra term H_f given by

$$H_f = \left(\sum_{\boldsymbol{z} \in \mathcal{N}_h \cap (\Gamma_s \cup \Gamma_D)} \sum_{T \subset \omega_{\boldsymbol{z}}} \alpha_T^{-1} h_T^2 \|f\|_{0,T}^2 + \sum_{\boldsymbol{z} \in \mathcal{N}_h \setminus (\Gamma_s \cup \Gamma_D)} \sum_{T \subset \omega_{\boldsymbol{z}}} \alpha_T^{-1} h_T^2 \|f - \bar{f}_{\omega_{\boldsymbol{z}}}\|_{0,T}^2 \right)^{1/2} \tag{3.2}$$

for the $P1$ conforming/nonconforming FEMs (the second term is a higher-order term for $f \in L^2(\Omega)$ and so is the first term for $f \in L^p(\Omega)$ with $p > 2$; see [3]) and

$$H_f = \left(\sum_{T \in \mathcal{T}_h} \alpha_T^{-1} h_T^2 \|f - \bar{f}_T\|_{0,T}^2 \right)^{1/2} \tag{3.3}$$

for the RT_0 mixed FEM.

Furthermore, without any assumption on the distribution of α, the following robust lower bound was established in [1, 2, 5]

$$\eta_e \leq C(\|\alpha^{-1/2}(\boldsymbol{\sigma} - \boldsymbol{\sigma}_h)\|_{0,\omega_e} + \underline{H}_f) \tag{3.4}$$

with the extra term $\underline{H}_f$ given by

$$\underline{H}_f = \left(\sum_{T \subset \omega_e} \alpha_T^{-1} h_T^2 \|f - \bar{f}_T\|_{0,T}^2 \right)^{1/2}$$

for the $P1$ conforming/nonconforming FEMs and

$$\underline{H}_f = 0$$

for the RT_0 mixed FEM.

While the discrete normal flux $\boldsymbol{\sigma}_h \cdot \boldsymbol{n}_e$ is constant on each edge e for all choices of $\boldsymbol{\sigma}_h$ given above, the discrete tangential derivative $\alpha^{-1}\boldsymbol{\sigma}_h \cdot \boldsymbol{t}_e$ is not constant on e for the RT_0 mixed FEM. Fortunately, in place of $\alpha^{-1}\boldsymbol{\sigma}_h \cdot \boldsymbol{t}_e$, one may use the nodal value of $\alpha^{-1}\boldsymbol{\sigma}_h \cdot \boldsymbol{t}_e$ at the midpoint $\boldsymbol{m}_e$ of the edge e and modify η_E as

$$\widetilde{\eta}_E = \left(\sum_{e \in \mathcal{E}_h} \widetilde{\eta}_e^2 \right)^{1/2} \tag{3.5}$$

with the local contributions

$$\widetilde{\eta}_e^2 = \begin{cases} \dfrac{2}{\alpha_{T_e^+}+\alpha_{T_e^-}} h_e \|[\![\boldsymbol{\sigma}_h \cdot \boldsymbol{n}_e]\!]\|_{0,e}^2 + \dfrac{2\alpha_{T_e^+}\alpha_{T_e^-}}{\alpha_{T_e^+}+\alpha_{T_e^-}} h_e \|[\![\alpha^{-1}\boldsymbol{\sigma}_h(\boldsymbol{m}_e)\cdot \boldsymbol{t}_e]\!]\|_{0,e}^2 & \text{for } e \subset \Omega, \\ \alpha_{T_e} h_e \|(\alpha^{-1}\boldsymbol{\sigma}_h)|_{T_e}(\boldsymbol{m}_e)\cdot \boldsymbol{t}_e - \frac{du_D}{ds}\|_{0,e}^2 & \text{for } e \subset \Gamma_D, \\ \alpha_{T_e}^{-1} h_e \|\boldsymbol{\sigma}_h|_{T_e}\cdot \boldsymbol{n}_e - g_N\|_{0,e}^2 & \text{for } e \subset \Gamma_N. \end{cases}$$

Such a modification only entails a higher order perturbation and thus does not affect the global upper bound (3.1) and the local lower bound (3.4), which is stated in the following theorem.

Theorem 3.1. *Let $\boldsymbol{\sigma}_h = \boldsymbol{\sigma}_h^m$ be the vector solution of the RT_0 mixed FEM (2.3). Then we have $\widetilde{\eta}_e \le \eta_e$ for all $e \in \mathcal{E}_h$ and*

$$\eta_E \le \widetilde{\eta}_E + C\widetilde{H}_f,$$

where the extra term $\widetilde{H}_f$ is the sum of (3.2) *and* (3.3)*.*

Proof. Following the proof of [13, Theorem 7.1], we can see that

$$h_e\|[\![\alpha^{-1}\boldsymbol{\sigma}_h\cdot\boldsymbol{t}_e]\!]\|_{0,e}^2 = h_e\|[\![\alpha^{-1}\boldsymbol{\sigma}_h(\boldsymbol{m}_e)\cdot\boldsymbol{t}_e]\!]\|_{0,e}^2 + \frac{1}{48}h_e^3\|[\![\alpha^{-1}\bar{f}_h]\!]\|_{0,e}^2$$

for every edge $e \subset \Omega$ and

$$h_e\|\alpha^{-1}\boldsymbol{\sigma}_h\cdot\boldsymbol{t} - \tfrac{du_D}{ds}\|_{0,e}^2 = h_e\|(\alpha^{-1}\boldsymbol{\sigma}_h)|_{T_e}(\boldsymbol{m}_e)\cdot\boldsymbol{t}_e - \tfrac{du_D}{ds}\|_{0,e}^2 + \frac{1}{48}h_e^3\|\alpha_{T_e}^{-1}\bar{f}_{T_e}\|_{0,e}^2$$

for every edge $e \subset \Gamma_D$. This immediately gives $\widetilde{\eta}_e \le \eta_e$ for all $e \in \mathcal{E}_h$.

To prove the second result, it is sufficient to show that

$$\sum_{e\subset\Omega}\frac{\alpha_{T_e^+}\alpha_{T_e^-}}{\alpha_{T_e^+}+\alpha_{T_e^-}}h_e^3\|[\![\alpha^{-1}\bar{f}_h]\!]\|_{0,e}^2 + \sum_{e\subset\Gamma_D}\alpha_{T_e}h_e^3\|\alpha_{T_e}^{-1}\bar{f}_{T_e}\|_{0,e}^2 \le C\widetilde{H}_f^2.$$

By using the inequality $\frac{\alpha_{T_e^+}\alpha_{T_e^-}}{\alpha_{T_e^+}+\alpha_{T_e^-}} \le \min\{\alpha_{T_e^+},\alpha_{T_e^-}\}$, we easily obtain for the edges $e \subset \Gamma_s \cup \Gamma_D$

$$\begin{aligned} &\sum_{e\subset\Gamma_s}\frac{\alpha_{T_e^+}\alpha_{T_e^-}}{\alpha_{T_e^+}+\alpha_{T_e^-}}h_e^3\|[\![\alpha^{-1}\bar{f}_h]\!]\|_{0,e}^2 + \sum_{e\subset\Gamma_D}\alpha_{T_e}h_e^3\|\alpha_{T_e}^{-1}\bar{f}_{T_e}\|_{0,e}^2 \\ &\le C\sum_{e\subset\Gamma_s\cup\Gamma_D}\sum_{T\subset\omega_e}\alpha_T h_e^3\|\alpha_T^{-1}\bar{f}_T\|_{0,e}^2 \le C\sum_{\boldsymbol{z}\in\mathcal{N}_h\cap(\Gamma_s\cup\Gamma_D)}\sum_{T\subset\omega_{\boldsymbol{z}}}\alpha_T^{-1}h_T^2\|f\|_{0,T}^2. \end{aligned} \tag{3.6}$$

For the remaining edges $e \subset \Omega\setminus\Gamma_s$, we have $\alpha_{T_e^+} = \alpha_{T_e^-}$ and thus it follows that

$$\begin{aligned} \sum_{e\subset\Omega\setminus\Gamma_s}\frac{\alpha_{T_e^+}\alpha_{T_e^-}}{\alpha_{T_e^+}+\alpha_{T_e^-}}h_e^3\|[\![\alpha^{-1}\bar{f}_h]\!]\|_{0,e}^2 &= \frac{1}{2}\sum_{e\subset\Omega\setminus\Gamma_s}\alpha_{T_e^+}^{-1}h_e^3\|[\![\bar{f}_h]\!]\|_{0,e}^2 \\ &\le C\sum_{\boldsymbol{z}\in\mathcal{N}_h\setminus(\Gamma_s\cup\Gamma_D)}\sum_{e\subset\omega_{\boldsymbol{z}}\setminus\partial\omega_{\boldsymbol{z}}}\alpha_{T_e^+}^{-1}h_e^3\|[\![\bar{f}_h]\!]\|_{0,e}^2. \end{aligned}$$

For each vertex $\boldsymbol{z} \in \mathcal{N}_h \setminus (\Gamma_s \cup \Gamma_D)$, we further obtain

$$\sum_{e \subset \omega_{\boldsymbol{z}} \setminus \partial\omega_{\boldsymbol{z}}} \alpha_{T_e^+}^{-1} h_e^3 \|[\![\bar{f}_h]\!]\|_{0,e}^2 = \sum_{e \subset \omega_{\boldsymbol{z}} \setminus \partial\omega_{\boldsymbol{z}}} \alpha_{T_e^+}^{-1} h_e^3 \|[\![\bar{f}_h - \bar{f}_{\omega_{\boldsymbol{z}}}]\!]\|_{0,e}^2 \leq C \sum_{T \subset \omega_{\boldsymbol{z}}} \alpha_T^{-1} h_T^2 \|\bar{f}_T - \bar{f}_{\omega_{\boldsymbol{z}}}\|_{0,T}^2,$$

which yields

$$\sum_{e \subset \Omega \setminus \Gamma_s} \frac{\alpha_{T_e^+}\alpha_{T_e^-}}{\alpha_{T_e^+} + \alpha_{T_e^-}} h_e^3 \|[\![\alpha^{-1}\bar{f}_h]\!]\|_{0,e}^2 \leq C \sum_{\boldsymbol{z} \in \mathcal{N}_h \setminus (\Gamma_s \cup \Gamma_D)} \sum_{T \subset \omega_{\boldsymbol{z}}} \alpha_T^{-1} h_T^2 \|f - \bar{f}_{\omega_{\boldsymbol{z}}}\|_{0,T}^2 + C \sum_{T \in \mathcal{T}_h} \alpha_T^{-1} h_T^2 \|f - \bar{f}_T\|_{0,T}^2. \quad (3.7)$$

The proof is completed by combining (3.6) and (3.7). □

4. Recovery-based Error Estimator

In this section we present and analyze an error estimator based on flux recovery which is applicable to the $P1$ conforming/nonconforming FEMs and the RT_0 mixed FEM in a unified way for the interface problem (1.1)–(1.2). The flux recovery procedure given below is an extension of the gradient recovery by *averaging at midpoints of edges* discussed in [8, 9, 10, 11] to the case of piecewise constant diffusion coefficients.

Suppose that the flux approximation $\boldsymbol{\sigma}_h \approx \boldsymbol{\sigma} = \alpha\nabla u$ has been obtained from one of the three lowest-order FEMs as given in the previous section. Then we recover a *weakly continuous piecewise linear* polynomial $R(\boldsymbol{\sigma}_h) \approx \boldsymbol{\sigma}$ by interpolating the following nodal values at midpoints of edges of $\mathcal{T}_h$.

Definition 4.1. *For an interior edge $e \subset \Omega$, the normal component of $R(\boldsymbol{\sigma}_h)$ at the midpoint $\boldsymbol{m}_e$ of e is uniquely determined by*

$$R(\boldsymbol{\sigma}_h)(\boldsymbol{m}_e) \cdot \boldsymbol{n}_e = \gamma_e^+ (\boldsymbol{\sigma}_h|_{T_e^+} \cdot \boldsymbol{n}_e) + \gamma_e^- (\boldsymbol{\sigma}_h|_{T_e^-} \cdot \boldsymbol{n}_e)$$

and the tangential component of $R(\boldsymbol{\sigma}_h)$ at the midpoint $\boldsymbol{m}_e$ is double-valued by

$$R(\boldsymbol{\sigma}_h)|_{T_e^\pm}(\boldsymbol{m}_e) \cdot \boldsymbol{t}_e = \alpha_{T_e^\pm} \big\{ \gamma_e^- (\alpha^{-1}\boldsymbol{\sigma}_h)|_{T_e^+}(\boldsymbol{m}_e) \cdot \boldsymbol{t}_e + \gamma_e^+ (\alpha^{-1}\boldsymbol{\sigma}_h)|_{T_e^-}(\boldsymbol{m}_e) \cdot \boldsymbol{t}_e \big\},$$

where the weight factors $\gamma_e^\pm$ are given by

$$\gamma_e^+ = \frac{\alpha_{T_e^-}^{1/2}}{\alpha_{T_e^+}^{1/2} + \alpha_{T_e^-}^{1/2}}, \qquad \gamma_e^- = 1 - \gamma_e^+ = \frac{\alpha_{T_e^+}^{1/2}}{\alpha_{T_e^+}^{1/2} + \alpha_{T_e^-}^{1/2}}. \quad (4.1)$$

For a boundary edge $e \subset \partial\Omega$, we set

$$R(\boldsymbol{\sigma}_h)(\boldsymbol{m}_e) \cdot \boldsymbol{n}_e = \begin{cases} \boldsymbol{\sigma}_h|_{T_e} \cdot \boldsymbol{n}_e & \text{for } e \subset \Gamma_D, \\ g_N & \text{for } e \subset \Gamma_N, \end{cases}$$

and

$$R(\boldsymbol{\sigma}_h)(\boldsymbol{m}_e)\cdot\boldsymbol{t}_e=\begin{cases}\alpha_{T_e}\frac{du_D}{ds} & \text{for } e\subset\Gamma_D,\\ \boldsymbol{\sigma}_h|_{T_e}(\boldsymbol{m}_e)\cdot\boldsymbol{t}_e & \text{for } e\subset\Gamma_N.\end{cases}$$

Finally, we find $R(\boldsymbol{\sigma}_h)|_T\in(\mathbb{P}_1(T))^2$ locally on each element $T\in\mathcal{T}_h$ which interpolates the normal and tangential components defined above.

In other words, the normal component of $R(\boldsymbol{\sigma}_h)$ is recovered at the midpoint $\boldsymbol{m}_e$ of an interior edge e by averaging the discrete normal fluxes $\boldsymbol{\sigma}_h|_{T_e^\pm}\cdot\boldsymbol{n}_e$, whereas the tangential component of $R(\boldsymbol{\sigma}_h)$ is recovered at $\boldsymbol{m}_e$ by first averaging the discrete tangential derivatives $(\alpha^{-1}\boldsymbol{\sigma}_h)|_{T_e^\pm}\cdot\boldsymbol{t}_e$ at $\boldsymbol{m}_e$ and then multiplying the result by the coefficient α. This ensures that both the normal component of $R(\boldsymbol{\sigma}_h)$ and the tangential component of $\alpha^{-1}R(\boldsymbol{\sigma}_h)$ are continuous at the midpoints of edges of $\mathcal{T}_h$. But, in general, it holds that $R(\boldsymbol{\sigma}_h)\notin H(\mathrm{div};\Omega)$ and $\alpha^{-1}R(\boldsymbol{\sigma}_h)\notin H(\mathrm{curl};\Omega)$.

Remark 4.2. *For a smooth coefficient α, the weight factors $\gamma_e^\pm$ are equal to $\frac{1}{2}$ and we get a single formula*

$$R(\boldsymbol{\sigma}_h)(\boldsymbol{m}_e)=\frac{1}{2}\big\{\boldsymbol{\sigma}_h|_{T_e^+}(\boldsymbol{m}_e)+\boldsymbol{\sigma}_h|_{T_e^-}(\boldsymbol{m}_e)\big\}$$

for every interior edge e. This recovery formula (with some modifications for boundary edges) was discussed in [8, 9] *for the $P1$ conforming FEM, in* [10] *for the $RT0$ mixed FEM, and recently in* [11] *for the $P1$ nonconforming FEM. In particular, it was shown to be superconvergent if the triangulations are uniform and the exact solution u is smooth. Numerical results reported in the next section suggest that superconvergence of $R(\boldsymbol{\sigma}_h)$ may be retained even when α is discontinuous.*

Remark 4.3. *The idea of averaging discrete normal fluxes on edges for flux recovery and averaging discrete tangential derivatives on edges for gradient recovery with the same weights (4.1) was also used by Cai and Zhang* [4, 5]*, but their recovery procedure is different from ours. They considered discontinuities of discrete normal fluxes and discrete tangential derivatives on edges separately by recovering two vector fields*

$$\widehat{\boldsymbol{\sigma}}_h\approx\boldsymbol{\sigma}=\alpha\nabla u\in H(\mathrm{div};\Omega)\quad\text{and}\quad\widehat{\boldsymbol{\rho}}_h\approx\nabla u\in H(\mathrm{curl};\Omega)$$

in conforming finite elements of $H(\mathrm{div};\Omega)$ and $H(\mathrm{curl};\Omega)$, respectively. Actually, one can set $\widehat{\boldsymbol{\rho}}_h=\nabla u_h^c$ for the $P1$ conforming FEM and $\widehat{\boldsymbol{\sigma}}_h=\boldsymbol{\sigma}_h^m$ for the RT_0 mixed FEM so that only one recovery is necessary for these two FEMs.

Definition 4.4. *The error estimator based on the flux recovery $R(\boldsymbol{\sigma}_h)$ is defined as*

$$\eta_R=\|\alpha^{-1/2}(\boldsymbol{\sigma}_h-R(\boldsymbol{\sigma}_h))\|_{0,\Omega}.$$

The following theorem reveals that the recovery-based error estimator η_R is in fact the edge residual error estimator (3.5) with slightly modified weight factors.

Theorem 4.5. *For every element $T \in \mathcal{T}_h$, we have*

$$\|\alpha^{-1/2}(\boldsymbol{\sigma}_h - R(\boldsymbol{\sigma}_h))\|_{0,T} = \left(\frac{|T|}{3}\sum_{e\subset\partial T}\widehat{\eta}_e^2\right)^{1/2},$$

where

$$\widehat{\eta}_e^2 = \begin{cases} \dfrac{1}{(\alpha_{T_e^+}^{1/2}+\alpha_{T_e^-}^{1/2})^2}\big|[\![\boldsymbol{\sigma}_h\cdot\boldsymbol{n}_e]\!]_e\big|^2 + \dfrac{\alpha_{T_e^+}\alpha_{T_e^-}}{(\alpha_{T_e^+}^{1/2}+\alpha_{T_e^-}^{1/2})^2}\big|[\![\alpha^{-1}\boldsymbol{\sigma}_h(\boldsymbol{m}_e)\cdot\boldsymbol{t}_e]\!]_e\big|^2 & \text{for } e\subset\Omega, \\ \alpha_{T_e}\big|(\alpha^{-1}\boldsymbol{\sigma}_h)|_{T_e}(\boldsymbol{m}_e)\cdot\boldsymbol{t}_e - \frac{du_D}{ds}\big|^2 & \text{for } e\subset\Gamma_D, \\ \alpha_{T_e}^{-1}\big|\boldsymbol{\sigma}_h|_{T_e}\cdot\boldsymbol{n}_e - g_N\big|^2 & \text{for } e\subset\Gamma_N. \end{cases}$$

Proof. Fix an edge $e\subset\partial T$ and set

$$\boldsymbol{\sigma}_h|_T(\boldsymbol{m}_e) - R(\boldsymbol{\sigma}_h)|_T(\boldsymbol{m}_e) = A_e\boldsymbol{n}_e + B_e\boldsymbol{t}_e,$$

where

$$A_e = \boldsymbol{\sigma}_h|_T\cdot\boldsymbol{n}_e - R(\boldsymbol{\sigma}_h)|_T(\boldsymbol{m}_e)\cdot\boldsymbol{n}_e,$$
$$B_e = \boldsymbol{\sigma}_h|_T(\boldsymbol{m}_e)\cdot\boldsymbol{t}_e - R(\boldsymbol{\sigma}_h)|_T(\boldsymbol{m}_e)\cdot\boldsymbol{t}_e.$$

Since $\boldsymbol{\sigma}_h - R(\boldsymbol{\sigma}_h)$ is a linear polynomial on T, we obtain

$$\begin{aligned}\|\alpha^{-1/2}(\boldsymbol{\sigma}_h - R(\boldsymbol{\sigma}_h))\|_{0,T}^2 &= \frac{|T|}{3}\sum_{e\subset\partial T}\alpha_T^{-1}\big|\boldsymbol{\sigma}_h|_T(\boldsymbol{m}_e) - R(\boldsymbol{\sigma}_h)|_T(\boldsymbol{m}_e)\big|^2 \\ &= \frac{|T|}{3}\sum_{e\subset\partial T}\alpha_T^{-1}(|A_e|^2+|B_e|^2). \end{aligned} \tag{4.2}$$

If e is an interior edge and $T = T_e^+$, then it follows by Definition 4.1 that

$$A_e = \gamma_e^-[\![\boldsymbol{\sigma}_h\cdot\boldsymbol{n}_e]\!]_e, \qquad B_e = \alpha_{T_e^+}\gamma_e^+[\![\alpha^{-1}\boldsymbol{\sigma}_h(\boldsymbol{m}_e)\cdot\boldsymbol{t}_e]\!]_e,$$

which leads to

$$\begin{aligned}\alpha_T^{-1}(|A_e|^2+|B_e|^2) &= \alpha_{T_e^+}^{-1}(\gamma_e^-)^2\big|[\![\boldsymbol{\sigma}_h\cdot\boldsymbol{n}_e]\!]_e\big|^2 + \alpha_{T_e^+}(\gamma_e^+)^2\big|[\![\alpha^{-1}\boldsymbol{\sigma}_h(\boldsymbol{m}_e)\cdot\boldsymbol{t}_e]\!]_e\big|^2 \\ &= \frac{1}{(\alpha_{T_e^+}^{1/2}+\alpha_{T_e^-}^{1/2})^2}\big|[\![\boldsymbol{\sigma}_h\cdot\boldsymbol{n}_e]\!]_e\big|^2 + \frac{\alpha_{T_e^+}\alpha_{T_e^-}}{(\alpha_{T_e^+}^{1/2}+\alpha_{T_e^-}^{1/2})^2}\big|[\![\alpha^{-1}\boldsymbol{\sigma}_h(\boldsymbol{m}_e)\cdot\boldsymbol{t}_e]\!]_e\big|^2. \end{aligned}$$

We also arrive at the same result when $T = T_e^-$ by exchanging the roles of T_e^+ and T_e^-. Besides, Definition 4.1 immediately gives

$$A_e = 0, \qquad B_e = \boldsymbol{\sigma}_h|_{T_e}(\boldsymbol{m}_e)\cdot\boldsymbol{t}_e - \alpha_{T_e}\frac{du_D}{ds} \qquad \forall e\subset\Gamma_D$$

and

$$A_e = \boldsymbol{\sigma}_h|_{T_e}\cdot\boldsymbol{n}_e - g_N, \qquad B_e = 0 \qquad \forall e\subset\Gamma_N.$$

Collecting the above results, we conclude that for every edge $e \subset \partial T$,

$$\alpha_T^{-1}(|A_e|^2 + |B_e|^2) = \widehat{\eta}_e^2,$$

which completes the proof by (4.2). □

It is trivial to see that $\frac{|T|}{3}\widehat{\eta}_e^2$ is equivalent to $\widetilde{\eta}_e^2$ independently of the mesh size h and the jumps of α between subdomains. Therefore the recovery-based error estimator η_R is robust with respect to the jumps of α between subdomains under the monotonicity condition stated in Section 3. By Theorem 4.5 it is also as inexpensive as the edge error residual estimators η_E and $\widetilde{\eta}_E$. Moreover, we expect that η_R will yield more accurate estimates of the numerical error $\|\alpha^{-1/2}(\boldsymbol{\sigma} - \boldsymbol{\sigma}_h)\|_{0,\Omega}$ than η_E and $\widetilde{\eta}_E$, due to the superconvergence property of the recovered flux $R(\boldsymbol{\sigma}_h)$ for smooth α.

5. NUMERICAL RESULTS

In this section we report some numerical results which illustrate the performance of the recovery-based error estimator η_R computed as in Theorem 4.5. The test problem is chosen to be the well-known benchmark problem with two intersecting interfaces and $f \equiv 0$ which was given by Kellogg [14]. Numerical experiments are carried out for the $P1$ conforming and nonconforming FEMs, because we have $\alpha\nabla_h u_h^{nc} = \boldsymbol{\sigma}_h^m$ when $f \equiv 0$ and α is piecewise constant over $\mathcal{T}_h$,.

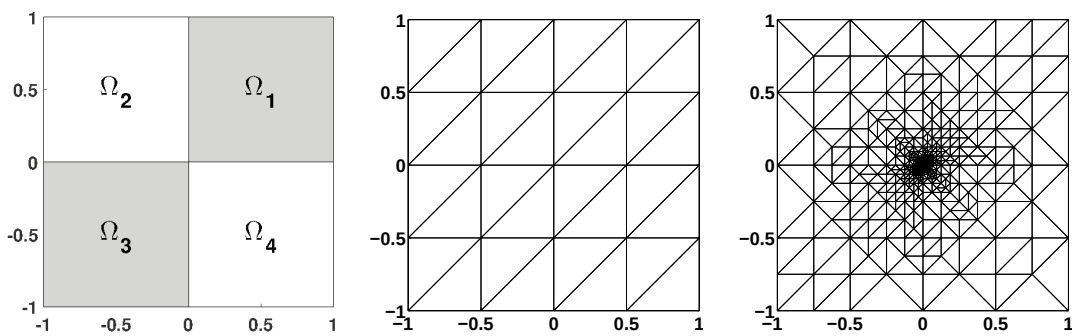

FIGURE 1. Subdomains (left), initial mesh (middle), and adapted mesh with 2484 elements for $\beta = 0.1$ (right).

Let $\Omega = (-1, 1)^2$ be divided into four subdomains $\{\Omega_i\}_{i=1}^4$ as shown in the left of Figure 1. For a given value of $0 < \beta < 2$ and $\rho = \frac{\pi}{4}$, the coefficient α is equal to

$$\alpha|_{\Omega_1} = \alpha|_{\Omega_3} = R = \frac{1}{\tan^2(\rho\beta)}, \qquad \alpha|_{\Omega_2} = \alpha|_{\Omega_4} = 1.$$

Notice that α is highly discontinuous between subdomains when β is close to 0 or 2. The exact solution has the form $u(r,\theta) = r^\beta \psi(\theta)$ in polar coordinates, where

$$\psi(\theta) = \begin{cases} \cos((\theta-\rho)\beta)/\cos(\rho\beta) & \text{if } 0 \le \theta \le \frac{\pi}{2}, \\ -\sin((\theta-3\rho)\beta)/\sin(\rho\beta) & \text{if } \frac{\pi}{2} \le \theta \le \pi, \\ -\cos((\theta-5\rho)\beta)/\cos(\rho\beta) & \text{if } \pi \le \theta \le \frac{3\pi}{2}, \\ \sin((\theta-7\rho)\beta)/\sin(\rho\beta) & \text{if } \frac{3\pi}{2} \le \theta \le 2\pi. \end{cases}$$

The Dirichlet condition determined by $u(r,\theta)$ is imposed on the whole boundary $\partial\Omega$. The solution u and the normal flux $\boldsymbol{\sigma} \cdot \boldsymbol{n}$ are continuous across subdomain interfaces. Moreover, it holds that $u|_{\Omega_i} \in H^{1+\beta-\epsilon}(\Omega_i)$ for any $\epsilon > 0$ on each subdomain Ω_i.

We consider two values $\beta = 1.9$ and $\beta = 0.1$, which correspond to $R = 0.006194\cdots$ and $R = 161.4476\cdots$, respectively. The coefficient α has the same jumps between subdomains, but the solution u is regular for $\beta = 1.9$, while it is singular around the origin for $\beta = 0.1$. Hence we perform uniform mesh refinement for $\beta = 1.9$ and adaptive mesh refinement for $\beta = 0.1$, starting with the coarse mesh of 32 congruent elements shown in the middle of Figure 1.

For $\beta = 0.1$, the sequence of adapted meshes is generated by applying the red-green-blue refinement for the $P1$ nonconforming FEM, where we mark the element $T \in \mathcal{T}_h$ for refinement if

$$\eta_T > 0.5 \max_{T' \in \mathcal{T}_h} \eta_{T'}, \qquad \eta_T = \|\alpha^{-1/2}(\boldsymbol{\sigma}_h - R(\boldsymbol{\sigma}_h))\|_{0,T}.$$

Numerical results for the $P1$ conforming FEM are obtained on the same sequence of adapted meshes. In the right of Figure 1, we show the adapted mesh with 2484 elements. It is clearly seen that the mesh is highly refined around the singularity of u.

In Tables 1–2, we present numerical errors and effectivity indices with respect to the horizontal edge length h_{el} for uniformly refined meshes and the number of elements N_{el} for adaptively refined meshes. The effectivity index EI is the ratio of the numerical error to the estimated error η_R. The numerical error is computed by the formula

$$\|\alpha^{1/2}\nabla(u - u_h^c)\|_{0,\Omega}^2 = \int_{\partial\Omega} \alpha \nabla u \cdot \boldsymbol{n}\,(u - 2u_h^c)\,ds + \|\alpha^{1/2}\nabla u_h^c\|_{0,\Omega}^2$$

for the $P1$ conforming FEM and

$$\|\alpha^{1/2}\nabla_h(u - u_h^{nc})\|_{0,\Omega}^2 = \int_{\partial\Omega} \alpha \nabla(u - 2u_h^{nc}) \cdot \boldsymbol{n}\, u\, ds + \|\alpha^{1/2}\nabla_h u_h^{nc}\|_{0,\Omega}^2$$

for the $P1$ nonconforming FEM, where a high-order quadrature is used to approximate the boundary integral over each edge $e \subset \partial\Omega$. These error formulas are readily derived using integration by parts and the equality $\nabla \cdot (\alpha \nabla u) = \nabla \cdot (\alpha \nabla_h u_h^{nc}) = 0$.

From Table 1 we see that the recovery-based error estimator η_R is asymptotically exact, even though the coefficient α has large jumps between subdomains. (Recall that the triangulations are uniform and the solution u is regular for $\beta = 1.9$.) On the other hand, Table 2 shows that η_R produce rather accurate estimates of the numerical error even when the solution u is

TABLE 1. Numerical errors and effectivity indices for $\beta = 1.9$ on uniformly refined meshes, where h_{el} is the horizontal edge length.

	$P1$ conforming FEM		$P1$ nonconforming FEM	
$1/h_{el}$	$\|\alpha^{1/2}\nabla(u-u_h^c)\|_{0,\Omega}$	EI	$\|\alpha^{1/2}\nabla_h(u-u_h^{nc})\|_{0,\Omega}$	EI
4	8.916063e–1	0.894610	8.563063e–1	0.963739
8	4.460283e–1	0.948537	4.404250e–1	0.987265
16	2.230530e–1	0.974457	2.222061e–1	0.995995
32	1.115329e–1	0.987251	1.114087e–1	0.998795
64	5.576746e–2	0.993626	5.574964e–2	0.999647
128	2.788389e–2	0.996811	2.788137e–2	0.999899
256	1.394197e–2	0.998405	1.394162e–2	0.999971
512	6.970988e–3	0.999202	6.970949e–3	0.999991

TABLE 2. Numerical errors and effectivity indices for $\beta = 0.1$ on adaptively refined meshes, where N_{el} is the number of elements.

	$P1$ conforming FEM		$P1$ nonconforming FEM	
N_{el}	$\|\alpha^{1/2}\nabla(u-u_h^c)\|_{0,\Omega}$	EI	$\|\alpha^{1/2}\nabla_h(u-u_h^{nc})\|_{0,\Omega}$	EI
32	1.306996e+1	0.464103	6.287810e+0	0.375773
512	3.465470e+0	0.569798	3.169759e+0	0.648549
1088	1.929723e+0	0.832406	1.800292e+0	0.851513
2484	1.204094e+0	0.871031	1.097007e+0	0.909756
6260	7.355309e–1	0.881781	6.627787e–1	0.918832
16484	4.456168e–1	0.887230	4.069451e–1	0.913213
45792	2.638758e–1	0.890879	2.470452e–1	0.908657
129060	1.558867e–1	0.891111	1.483348e–1	0.904839
339124	9.543845e–2	0.892891	9.214557e–2	0.901201

very singular and highly non-uniform meshes are used. These numerical results illustrate the robustness of η_R and its superiority over the edge residual error estimators η_E and $\widetilde{\eta}_E$.

ACKNOWLEDGMENT

This study was supported by 2014 Research Grant from Kangwon National University(No. C1011748-01-01).

REFERENCES

[1] C. Bernardi and R. Verfürth, *Adaptive finite element methods for elliptic equations with non-smooth coefficients*, Numer. Math., **85** (2000), 579–608.
[2] M. Petzoldt, *A posteriori error estimators for elliptic equations with discontinuous coefficients*, Adv. Comput. Math., **16** (2002), 47–75.
[3] C. Carstensen and R. Verfürth, *Edge residuals dominate a posteriori error estimates for low order finite element methods*, SIAM J. Numer. Anal., **36** (1999), 1571–1587.
[4] Z. Cai and S. Zhang, *Recovery-based error estimator for interface problems: conforming linear elements*, SIAM J. Numer. Anal., **47** (2009), 2132–2156.
[5] Z. Cai and S. Zhang, *Recovery-based error estimators for interface problems: mixed and nonconforming finite elements*, SIAM J. Numer. Anal., **48** (2010), 30–52.
[6] O. C. Zienkiewicz and J. Z. Zhu, *A simple error estimator and adaptive procedure for practical engineering analysis*, Internat. J. Numer. Methods Engrg., **24** (1987), 337–357.
[7] C. Carstensen and S. Bartels, *Each averaging technique yields reliable a posteriori error control in FEM on unstructured grids. Part I: Low order conforming, nonconforming, and mixed FEM*, Math. Comp., **71** (2002), 945–969.
[8] G. Goodsell and J. R. Whiteman, *A unified treatment of superconvergent recovered gradient functions for piecewise linear finite element approximations*, Internat. J. Numer. Methods Engrg., **27** (1989), 469–481.
[9] N. Levine, *Superconvergent recovery of the gradient from piecewise linear finite-element approximations*, IMA J. Numer. Anal., **5** (1985), 407–427.
[10] J. H. Brandts, *Superconvergence and a posteriori error estimation for triangular mixed finite elements*, Numer. Math., **68** (1994), 311–324.
[11] J. Hu and R. Ma, *Superconvergence of both the Crouzeix–Raviart and Morley elements*, Numer. Math., **132** (2016), 491–509.
[12] K. Y. Kim, *A posteriori error analysis for locally conservative mixed methods*, Math. Comp., **76** (2007), 43–66.
[13] B. I. Wohlmuth and R. H. W. Hoppe, *A comparison of a posteriori error estimators for mixed finite element discretizations by Raviart–Thomas elements*, Math. Comp., **68** (1999), 1347–1378.
[14] R. B. Kellogg, *On the Poisson equation with intersecting interfaces*, Appl. Anal., **4** (1974), 101–129.